DIRECT DETERMINATION OF THE STRUCTURE OF BARIUM STEARATE MULTILAYERS BY X-RAY DIFFRACTION

W. LESSLAUER *and* J. K. BLASIE

From the Johnson Research Foundation, University of Pennsylvania, Philadelphia, Pennsylvania 19104

ABSTRACT Diffraction of X-rays is recorded from barium stearate multilayer systems with from 2 to 60 double layers or unit cells. The generalized Patterson function $P'(x)$ is calculated by an integral Fourier transform of observed intensity data from a specimen containing only two unit cells. The Patterson function $P_0(x)$ of a single unit cell is determined from $P'(x)$ and the electron density distribution of a bimolecular leaflet is obtained by a deconvolution procedure of $P_0(x)$ after Hosemann and Bagchi. The electron density distribution is also calculated independently by a conventional Fourier synthesis with an experimentally established set of phases. The results of the two methods are consistent and fit a physical model of the bimolecular leaflet. A direct analysis, therefore, can be performed if diffraction is observed from multilayer systems with a small number of unit cells.

INTRODUCTION

Current models for the structure of biological membranes propose that the lipids within the membranes are assembled in a three-dimensional arrangement which is generally referred to as a bimolecular leaflet. Whether this structure occupies the whole surface area of the membrane or whether there is a mosaic pattern of areas with different kinds of arrangements of the membrane components is an open question. There is evidence, however, that at least some membranes have a lipid hydrocarbon core. This is based on X-ray diffraction experiments (Schmitt et al., 1941; Gras and Worthington, 1969; Engelman, 1970) or differential scanning calorimetry (Steim et al., 1969), in addition to older experiments of Gorter and Grendel (1925) and Fricke (1925).

The structure of bimolecular lipid layers has been investigated in model systems by X-ray diffraction (Finean, 1953; Luzzati, 1968; Levine et al., 1968; Blaurock, 1970). Unit cell dimensions can easily be obtained from these experiments. The determination of the electron density distribution within the unit cell by a Fourier syn-

thesis, however, requires the knowledge of the phase angles. Indirect methods have been used in these studies to solve the phase problem. It is true, especially in the cases of biological membranes or their lipid model systems where the main problem is to establish the one-dimensional electron density distribution in the direction normal to the plane of the membrane, that a satisfactory solution usually can be found by guessing a phase combination on the basis of physical intuition. If the number of reflections to be used in the Fourier synthesis exceeds four or five, however, this method is a cumbersome procedure with unreliable results.

One way to achieve an experimental determination of the phase angles will be outlined in this report. It has been shown theoretically by Hosemann and Bagchi (1962) that a direct analysis of diffraction data can be performed if it is obtained from microcrystalline systems containing a small enough number of unit cells that the natural line shape of the interference function (James, 1965) can be observed. The underlying reason for this is that, under these circumstances, the square of the unit cell structure factor is "sampled" by the interference function over a finite region of reciprocal space about each point of the reciprocal lattice.

Evidence will be presented that these effects can be observed experimentally in diffraction from barium stearate multilayer systems. A fatty acid multilayer system was chosen because the unit cell presents the basic features of a bimolecular lipid leaflet, namely a hydrocarbon core between two regions of higher electron density, and because diffracting systems with a known number of unit cells can readily be obtained. The electron density distribution across the bimolecular leaflet will be derived on the basis of diffraction obtained from specimens with only two unit cells and compared with the results of a conventional Fourier synthesis for a specimen with a large number of unit cells.

MATERIALS AND METHODS

Stearic and other fatty acids were purchased from Applied Science Laboratories Inc. (State College, Pa.) in samples with a purity of better than 99%. Analytical grade reagents were used throughout. Organic solvents were redistilled before use.

"Multilayers" of barium stearate were prepared, as described by K. Blodgett (1935), by repeatedly dipping a support through a monomolecular film of stearate on the water surface of a Langmuir trough. The film was kept at constant surface pressure by a moving float (Sher and Chanley, 1955). The support consisted usually of a curved glass slide. A very thin silver mirror was evaporated onto the surface of the glass slide.

X-ray diffraction patterns were obtained with focusing cameras of the Franks' type (Elliot and Worthington, 1963). They were used with a Jarrel Ash microfocus X-ray unit (Ni-filtered CuKα-radiation) (Jarrell Ash Div., Fisher Scientific, Waltham, Mass.). The effective focal area on the anode was 1.4 mm $\times$ 5 μ. Diffraction patterns were recorded on Ilford Industrial G X-ray film (Ilford, Ltd., Ilford, England) employing cylindrical cassettes with a diameter of 62.5 or 125 mm. Most exposures were done in a camera equipped with a vacuum path. The specimen chamber had Melinex windows. The specimen could be kept at atmospheric pressure and equilibrated with a defined water vapor pressure during the exposure. A line source of X-rays was used to record the lamellar reflections. The specimen was aligned

parallel to the X-ray beam. The beam width at the guard slit was of the order of 100 μ. For exposures with a point-focused X-ray beam the beam had a diameter of 200 μ at the guard slits. Exposures with a point-focused X-ray beam were recorded with a flat plate cassette with a specimen-to-film distance of 10 mm. Densitometer tracings of the diffraction patterns were obtained on a Joyce, Loebl Mark III CS microdensitometer (Joyce, Loebl & Co., Inc., Burlington, Mass.).

Experiments were done at 28 $\pm$1°C.

Numerical computations were done on a PDP-6 computer of the Medical School Computer Facility, University of Pennsylvania.

RESULTS

The diffraction of X-rays from barium stearate multilayers was recorded for a range of specimens containing from 2 to 60 double layers or unit cells. The number of observed reflections arising from the lamellar stacking of the barium stearate layers

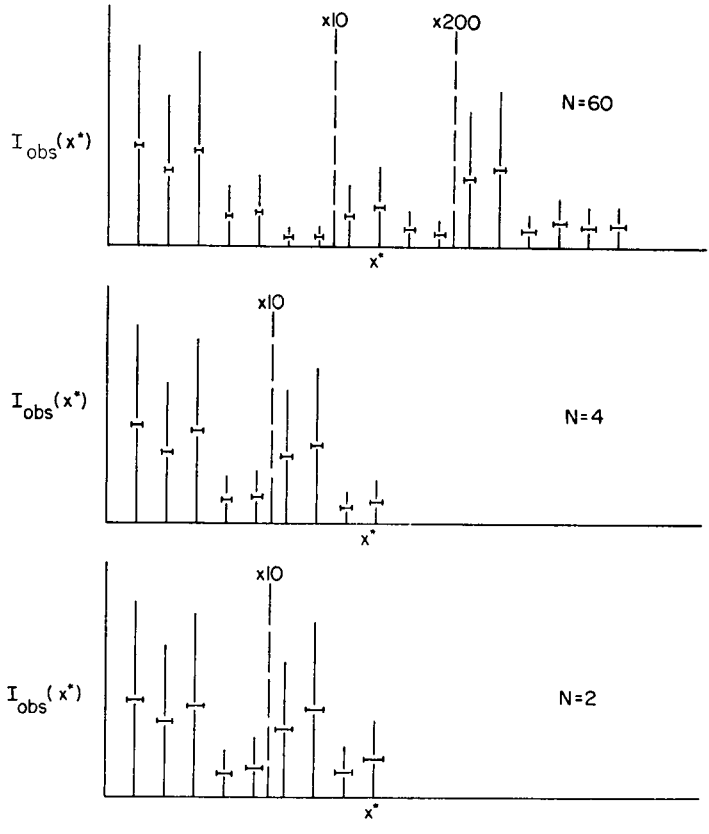

FIGURE 1 Schematic representation of the observed intensities $I_{obs}(x^*)$ of lamellar reflections from specimens with 2, 4, and 60 unit cells plotted in intervals of $1/D$. The half-width of the peaks is also given in units of $1/D$ where the scale for the half-width was expanded by a factor of three as compared with the spacing of the lamellar reflections. See Table I.

TABLE I

OBSERVED DIFFRACTED INTENSITIES, $I_{obs}(h)$, FOR SPECIMENS WITH N = 60, 4, AND 2 UNIT CELLS

h	$N = 60$		$N = 4$		$N = 2$	
	$I_{obs}(h)$	$\frac{\Delta p}{1/D}$	$I_{obs}(h)$	$\frac{\Delta p}{1/D}$	$I_{obs}(h)$	$\frac{\Delta p}{1/D}$
1	1000.0	0.088	1000.0	0.136	1000.0	(0.175)
2	749.0	0.083	710.0	0.143	700.0	0.175
3	968.0	0.083	935.0	0.138	850.0	0.178
4	305.0	0.078	236.0	0.146	219.0	0.170
5	356.0	0.083	272.0	0.143	275.0	0.179
6	93.0	0.088	68.1	0.143	62.5	0.198
7	103.0	0.098	78.8	0.143	81.3	0.210
8	30.5	0.098	16.1	0.148	22.5	0.222
9	40.0	0.102	21.5	0.148	33.8	0.247
10	18.0	0.146				
11	12.8	0.146				
12	3.4	0.146				
13	3.9	0.146				
14	0.8	0.170				
15	1.2	0.195				
16	0.5	0.195				
17	0.5	0.195				

For $N = 60$, the values represent integrated intensities. For $N = 4$, 2, the intensity at the ideal reciprocal lattice point h/D is given. The half-widths Δp of the reflections are in units of $1/D$.

(abbreviated "lamellar reflections") varied as a function of the number of unit cells of the diffracting specimen. The maximum number of lamellar reflections for specimens with 2 and 60 unit cells was 9 and 17, respectively (Fig. 1). Unit cell dimensions D were calculated from the lamellar reflections. Values obtained were $D = 47.0$ A for barium stearate, as compared with $D = 37.0$ A for barium myristate.

The half-width of individual lamellar reflections, defined as the width of the reflection at half the maximum intensity of its domain, was constant for the first few orders. A small and systematic increase in half-width with increasing order of the reflections was observed past the first five to seven reflections. This increase was less than 5% per order. Thus, for a given setup of the X-ray camera, the half-width of the reflections was found to have a characteristic value for a given specimen.

A systematic study was done to determine the influence of the number of unit cells in the diffracting specimen on the shape and half-width of the lamellar reflections. A clear broadening of the reflections was found in the diffraction from specimens with only a few unit cells. The half-width of the lamellar reflections from specimens with two unit cells was more than twice that from a specimen with 60 unit cells. It was found that the half-width decreased continuously with increasing number of unit cells for specimens with from 2 to 10 double layers. No further decrease in half-

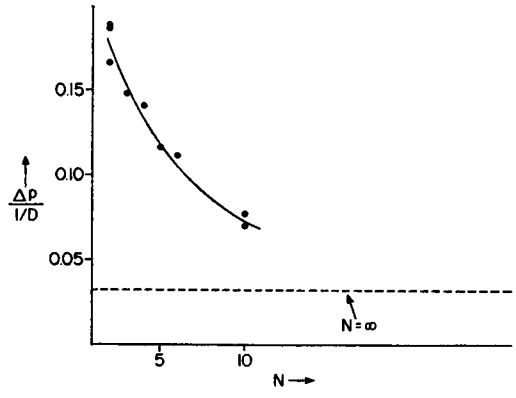

FIGURE 2 Half-width $\Delta p/(1/D)$ of lamellar reflections as a function of the number N of unit cells in the diffracting specimen in units of $1/D$. The width of the primary beam is also given in the same units ($N = \infty$).

width was observed with specimens containing more than 10 unit cells, although the half-width of the focused beam of the X-ray camera was still small compared with the half-width of the lamellar reflections (Fig. 2). The position of the maxima of the lamellar reflections in reciprocal space coincided in all instances with the ideally periodic reciprocal lattice points, regardless of the number of unit cells in the diffracting specimen.

No difference in spacing and relative intensities of the lamellar reflections was detected between the diffraction pattern of a specimen kept at 100% humidity during exposure and that of the same specimen reexposed at 0% humidity, even after exhaustive vacuum drying over P_2O_5 for a period of several days.

Diffraction patterns obtained from a multilayer specimen using a point-focused X-ray beam exhibited, in addition to the lamellar reflections, diffraction corresponding to a Bragg spacing of approximately 4.2 A. This reflection was situated along the equator if the axis of the lamellar reflections was defined as the meridian of the diffraction pattern. A spreading of this reflection off the equator was observed, and a clearly distinguishable off-equatorial spot was seen in the pattern.

DISCUSSION

The multilayered systems obtained by the method of K. Blodgett can be regarded as stacked arrays of plane monomolecular layers formed by the salts of fatty acids with divalent cations (e.g., barium stearate). Every other layer is overturned with respect to the preceding one, so that a plane of symmetry exists between two adjacent layers. The repeating unit D, along an axis normal to the plane of the stearate layers, therefore, consists of two adjacent monomolecular films. The following discussion is based on this symmetry of the structure.

It is assumed that the electron density distribution of the multilayer structure can

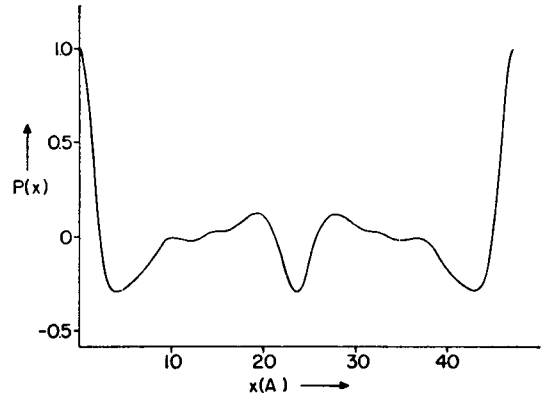

FIGURE 3 Patterson function $P(x)$ (in relative units) calculated with 17 lamellar reflections of a specimen with 60 unit cells. Normalization is for $P(0) = 1.0$.

be represented by a set of parallel and infinitely extended planes with uniform electron density in the plane. The one-dimensional electron density distribution (Blaurock and Worthington, 1966) along an x-axis perpendicular to the planes will be called $\rho(x)$. The electron density distribution $g(\mathbf{r})$ for the multilayer then becomes: $g(\mathbf{r}) = \text{const} \cdot \rho(x)$. The properties of the function $\rho(x)$ determine the characteristics of the lamellar reflections.

Diffraction Arising from Multilayers with a Large Number of Unit Cells

Up to 17 lamellar reflections are observed from a specimen with 60 unit cells. The position and relative intensities of the lamellar reflections are determined from microdensitometer tracings of the diffraction patterns. The Patterson function $P(x)$,

$$P(x) = \frac{2}{D} \cdot \sum_{h=1}^{h_{max}} h^2 \cdot I_{obs}(h) \cos\left(2\pi x \frac{h}{D}\right), \quad (1)$$

where $h^2 \cdot I_{obs}(h)$[1] is proportional to $|F(h)|^2$, can be calculated, whose resolution is limited by h_{max} (Fig. 3). The interpretation of $P(x)$, however, is hampered by the well-known fact that it contains overlapping contributions from adjacent unit cells.

A resolution-limited electron density distribution, $\rho'(x)$, can be reconstructed by a Fourier summation,

$$\rho'(x) = \frac{2}{D} \cdot \sum_{h=1}^{h_{max}} h \cdot \{\pm [I_{obs}(h)]^{1/2}\} \cdot \cos\left(2\pi x \frac{h}{D}\right). \quad (2)$$

[1] The observed intensities have to be corrected by a factor of h which arises from the geometrical arrangement of the curved specimen in the X-ray beam. A second factor of h is due to the divergence of the X-ray beam in diffraction from specimen with a large number of unit cells (Blaurock and Worthington, 1966). In the case of systems with a small number of unit cells, the beam divergence is small compared to the angular width of the reflection and this second factor of h is not required (Blaurock and Worthington, 1966).

For a centrosymmetric structure the phase problem is reduced to the choice between two possible angles, 0 or π. There are 2^h different functions $\rho'(x)$ which are, in principle, all equally probable. One has then to choose one of these possibilities after criteria which are often based on physical intuition. One such criterion in the case of stearate multilayers is that the correct $\rho'(x)$ should have regions nearly constant electron density whose extensions correspond to the chain length of —CH_2— groups of the fatty acids (criterion I). There are, however, ways to overcome the ambiguities involved when the phase angles are chosen on the basis of so-called indirect methods. If diffraction can be observed from systems with only a small number of unit cells, the information content of the diffraction pattern is higher than in the usual case of X-ray diffraction where the number of unit cells is, for practical purposes, infinite. It is the advantage of the method of K. Blodgett that diffracting systems with a precisely known and small number of unit cells can be built up.

Diffraction Arising from Multilayers with a Small Number of Unit Cells

The angular width ϵ of the domain of a reflection is inversely proportional to the number N of unit cells in the diffracting system,

$$\epsilon = \frac{1}{N \cdot D} . \tag{3}$$

If N is large, ϵ becomes small and the observed width and profile of a reflection are theoretically determined only by line width and profile of the primary beam of a given X-ray camera. For small values of N, however, the angular width of a reflection increases. A broadening of the reflection in the diffraction pattern can be observed if ϵ becomes larger than the line width of the primary beam of the X-ray camera. Such a broadening is observed in diffraction patterns from specimens with $N = 2, 3, \cdots, 6$ (Fig. 2). In the case of $N = 2$, the reflections are broad enough, as compared to the line width of the camera, that the primary beam can be treated to a good approximation as infinitely narrow. The observed half-width of a reflection depends then primarily on the half-width of the maxima of the interference function of the diffracting system. There is no further decrease in half-width when N is increased from 10 to 60, although the primary beam is still much narrower than the observed reflections from these specimens. A ready explanation is that not all of the 60 unit cells actually diffract coherently. The fact that the reflections from the 60 unit cell specimen are broader than expected cannot be attributed to simple disorder since 17 orders with a reasonably constant half-width are observed.

Shifts of the maxima of the reflections out of the ideal reciprocal lattice points resulting in asymmetric reflections are, in general, to be expected once the number of unit cells in the diffracting system is small enough that a broadening of the reflections can be observed. This is, of course, because of the fact that under these circumstances the square of the structure factor, $| F(x^*) |^2$, is sampled by the interference function

over a finite region in reciprocal space about the reciprocal lattice points. The fact that no such shifts can be detected in diffraction from barium stearate multilayers, even if the system is made up of only two unit cells, indicates that the Fourier transform of a single unit cell is a function oscillating in phase with the interference function everywhere in reciprocal space where diffraction is observed. The observation of a repeat distance of 47.0 A and of reflections arising from the packing of the hydrocarbon chains requires that the barium ions be lined up between the bimolecular lipid layers. The shifts to be observed, if the peaks of high relative electron density caused by the barium ions do not occur exactly at the edges of the unit cell, might be small for some reflections. Structure factor and interference function would then, however, have to get systematically out of phase and at least some reflections should fall on high enough slopes of the structure factor that a shift can be detected. The most probable combination of phase angles for the calculation of a Fourier synthesis, therefore, is an alternating sequence of π and 0 for the first to the ninth order (criterion II) since nine orders have been observed from a specimen with two unit cells. For this phase sequence, the origin is placed in the center of the bimolecular layer. This indicates that the dominant feature of the electron density distribution is a narrow region of high electron density at either edge of the unit cell, which is due to the barium ions. $\rho'(x)$ calculated by a Fourier synthesis with such an alternating phase sequence with 9 reflections from a specimen with 60 unit cells already shows this characteristic.

Furthermore, if structure factor and interference function get systematically out of phase, a reflection of much lower intensity than the neighboring reflections, or even a missing reflection, should occur at a certain reciprocal lattice point in diffraction patterns from specimen with many unit cells. Such phenomena can be observed with multilayers made from magnesium stearate, where drying experiments prove the existence of a small water space between the lipid layers (Lesslauer and Blasie, 1970), but not with barium stearate multilayers, even if 17 orders are observed. It is, therefore, to be expected, that the phase angles for reflections 9–17 follow the same alternating sequence of π and 0. $\rho'(x)$ calculated with this phase sequence and 17 lamellar reflections from a specimen with 60 unit cells is shown in Fig 4. The phase sequence of criterion II can be considered to be experimentally determined with a high degree of reliability. Furthermore, it can be shown by trial and error that $\rho'(x)$ obtained with this phase combination is the only solution which also satisfies criterion I, and it may be regarded as the correct solution. The inner region of the unit cell corresponds to the hydrocarbon core. It has a low and nearly constant electron density except for an approximately 3-A-wide trough in the center. This trough cannot be an artifact caused by limited resolution of the Fourier synthesis. It must be caused by the fact that the electron density of the region of the terminal —CH_3 groups in lower than that of the chain of —CH_2— groups. The layer of barium ions gives rise to the peak of high electron density at either edge of the unit cell. The minima immediately inside these peaks are in part due to truncation artifacts; however, one has to conclude that

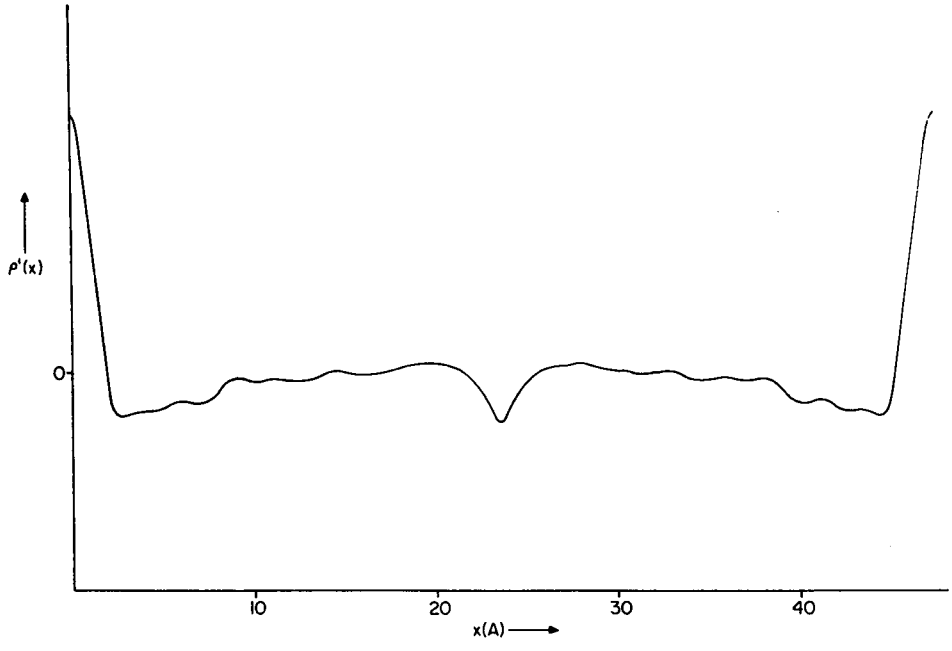

FIGURE 4 Electron density distribution $\rho'(x)$ for a single unit cell (in relative units), obtained by a Fourier summation with 17 lamellar reflections and an alternating phase sequence of $\pi, 0, \pi \ldots$.

adjacent to the layer of barium ions is a region whose electron density is slightly less than that of the —CH_2— chain. This may be due to the average angle of tilt of the hydrocarbon chains with the normal to the plane of the layers.

It was shown theoretically by Hosemann and Bagchi (1962) that a special kind of Patterson function, $P'(x)$, is derived if the observed intensity function, $I_{obs}(x^*)$, is obtained for a specimen containing a small enough number of unit cells that the line shape of the interference function can be observed. $P'(x)$ is defined by

$$P'(x) = 2 \cdot \int_0^\infty x^* \cdot I_{obs}(x^*) \cdot \cos(2\pi \cdot x \cdot x^*)\, dx^*, \tag{4}$$

where $x^* \cdot I_{obs}(x^*)$ (see footnote 1) is proportional to $|F(x^*)|^2$. To discuss the properties of $P'(x)$, the electron density distribution of the multilayer is expressed as

$$\rho(x) = \rho_0(x) * [z(x) \cdot s(x)]. \tag{5}$$

One may then write

$$P'(x) = \frac{1}{D} P_0(x) * \{z(x) \cdot [s(x) * s(x)]\}. \tag{6}$$

[$z(x)$ = lattice function; $s(x)$ = shape function; $\rho_0(x)$, $P_0(x)$ refers to a single unit cell.] It is apparent that $P'(x)$ is defined only in the interval $-N \cdot D \leq x \leq N \cdot D$. Furthermore, $P'(x)$ in the intervals $-N \cdot D \leq x \leq -(N-1) \cdot D$ and $(N-1) \cdot D \leq x \leq N \cdot D$ should correspond to $P_0(x)$. Hosemann and Bagchi (1962) originally showed that it is sufficient to use a linear approximation for $|F(x^*)|^2$ in the domain of each reflection to give $P'(x)$ these properties. This approximation cannot be used, however, for the system under discussion because

$$\text{grad} \mid F(x^*) \mid^2 = 0$$

in the domain of each reflection (criterion II). Higher order terms must be included and $P'(x)$ is calculated according to the complete expression 4.

$P'(x)$ calculated for the case of $N = 2$ and nine lamellar reflections is shown in Fig. 5. It is obvious from that figure that $P'(x)$ no longer is a periodic function like the conventional Patterson function $P(x)$. $P'(x)$ at $x = 2D$ has diminished to less than half its value at the origin. Theoretically, $P'(x)$ for $N = 2$ should be zero outside the interval from $-2D$ to $2D$. It is observed, however, that this condition is not ideally fulfilled. Though the values of $P'(x)$ become rapidly smaller outside of $\pm 2D$,

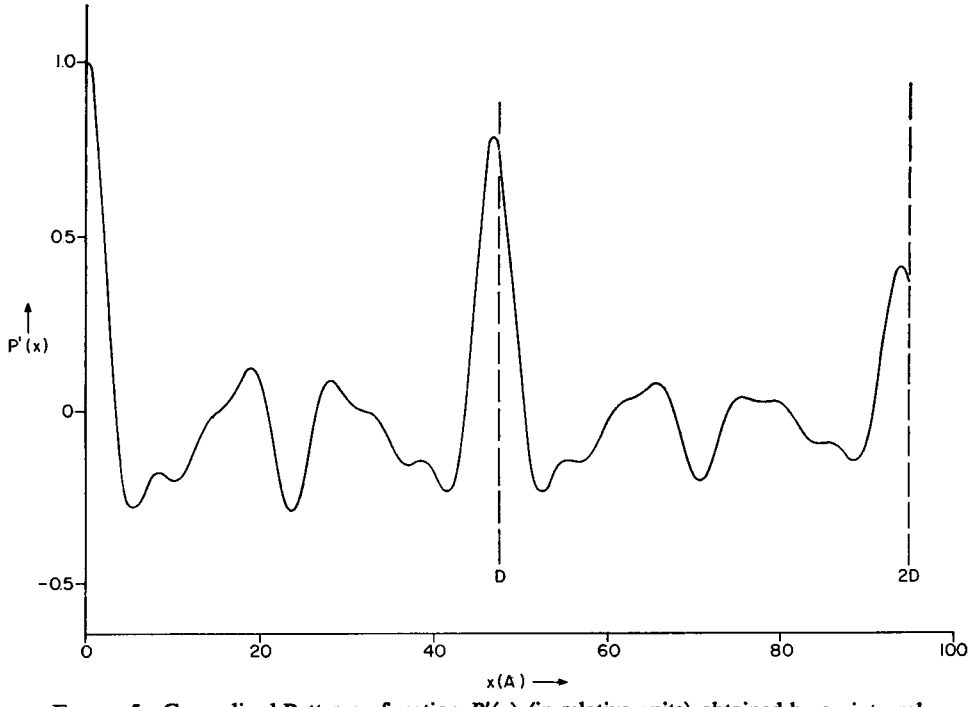

FIGURE 5 Generalized Patterson function $P'(x)$ (in relative units) obtained by an integral Fourier transformation of the observed intensity function from a specimen with two unit cells. The equivalent of nine lamellar reflections was used in the computation.

it remains nonzero in a space corresponding to one to two additional unit cell periods. Analogous results are obtained, if $P'(x)$ is calculated for specimens with three unit cells, where the function still has discernible maxima at $\pm 4\ D$ and $\pm 5\ D$.

Several reasons for this behavior can be discussed. $P'(x)$ must have a maximum near $\pm N \cdot D$, since $\rho_0(x)$ has a maximum at the edges of the unit cell. The given resolution, depending on the highest Bragg angle up to which diffraction has been observed, will determine how rapidly $P'(x)$ is dampened outside $\pm N \cdot D$. Disorder in the specimen will have the result that $s(x)$ is not exactly a step function with discontinuities at 0 and $N \cdot D$. The convolution product $s(x) * s(x)$, which terminates $P'(x)$ according to equation 6, may then exist outside of $\pm N \cdot D$. A less likely possibility is that in the process of building up the multilayer the number of layers deposited is not equal to the number of dippings of the specimen support through the monomolecular film. This situation could arise if the film on the water surface in the Langmuir trough is not a true monomolecular layer but contains regions where two or more layers are pushed on top of each other, e.g., when the film is compressed beyond collapse pressure. Great care has been taken to avoid this in the preparation of the specimen. Furthermore, such a random variation of the number of unit cells in the specimens would affect the reproducibility and consistency of the experimental results significantly, and this is not observed. It should be pointed out that the observed half-width of the lamellar reflections was, at least for $N = 2$, smaller than expected on a theoretical basis for a structure $\rho'(x)$ of Fig. 4. For $N = 2$ the observed intensity as a function of $(2 \sin \theta)/\lambda$ should correspond essentially to a $\cos^4(\pi \cdot D \cdot x^*)$ like function and a half-width ~ 0.35 is to be expected. This compares to an observed value of approximately 0.18. No ready explanation can be given for the discrepancy; it may be due in part to the nonlinearity in the response of the X-ray film used to record the diffraction patterns.

Despite these limitations the Patterson function for a single unit cell, $P_0(x)$, can be determined from $P'(x)$ (Hosemann and Bagchi; 1962), because $P'(x)$ is not an ideally periodic function (Fig. 5). The physical meaning of equation 6 is that $P'(x)$ may be represented by a convolution of $P_0(x)$ with a weighted lattice function. It appears then that for any x_i :

$$\begin{aligned} P'(x_i) &= \{P_0(x) * [\delta(x) \cdot \sigma(0)] + P_0(x) * [\delta(x - D) \cdot \sigma(D)]\}_{x_i} \\ &= P'(0) \cdot P_0(x_i) + P'(D) \cdot P_0(x_i - D); \\ P'(x_i - D) &= \{P_0(x) * [\delta(x) \cdot \sigma(0)] + P_0(x) * [\delta(x + D) \cdot \sigma(-D)]\}_{x_i - D} \\ &= P'(0) \cdot P_0(x_i - D) + P'(D) \cdot P_0(x_i); \\ & 0 \leq x_i \leq D; \quad \sigma(x) = s(x) * s(-x); \quad P'(x) = P' - x). \end{aligned} \tag{7}$$

Equations 7 can be solved for $P_0(x)$. $P_0(x)$ exists only in the interval $-D \leq x \leq D$ and is asymmetric in $0 \leq x \leq D$ and in $-D \leq x \leq 0$. $P_0(x)$ calculated for a specimen with $N = 2$ is shown in Fig. 6.

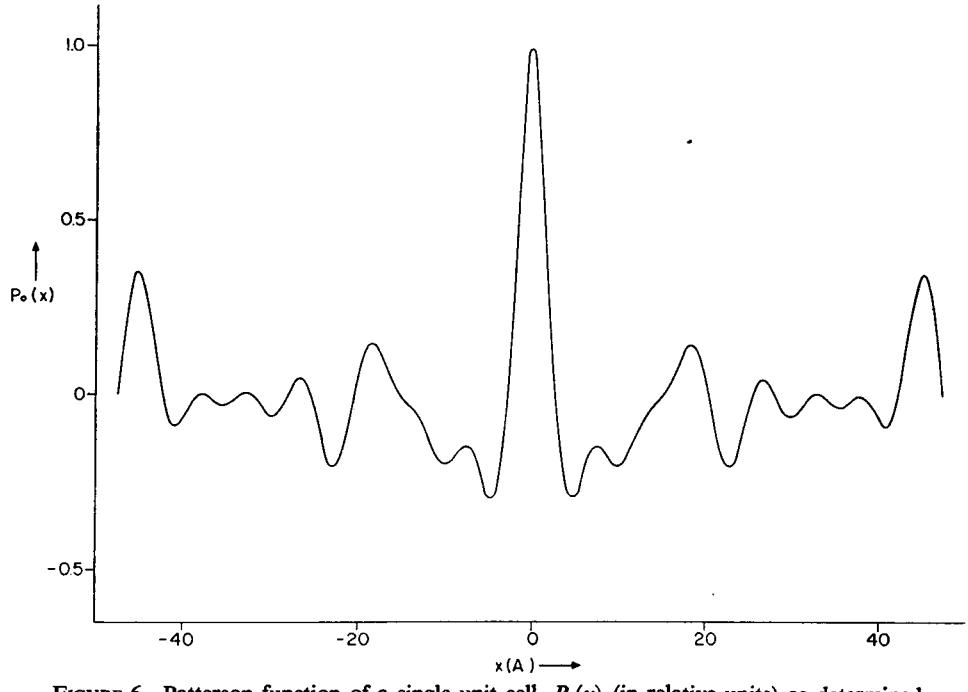

FIGURE 6 Patterson function of a single unit cell, $P_0(x)$ (in relative units) as determined from the generalized Patterson function.

Finally, $P_0(x)$ can be deconvoluted. According to Hosemann and Bagchi $P_0(x)$ and $\rho_0(x)$ are divided in small intervals Δx and two new functions $p(x)$ and $\mu(x)$ are defined

$$p(x) = \int_{x-\Delta x/2}^{x+\Delta x/2} P_0(u)\, du; \qquad \mu(x) = \int_{x-\Delta x/2}^{x+\Delta x/2} \rho_0(u)\, du \tag{8}$$

where Δx is small enough that $P_0(x)$ and $\rho_0(x)$ are constant in Δx. The electron density distribution $\mu(x)$ can be obtained by a deconvolution of $p(x)$ through a recursion process since in the one-dimensional case

$$p(-D + n\cdot\Delta x) = \sum_{i=0}^{n} \mu(i\cdot\Delta x)\cdot\mu(n\cdot\Delta x - i\cdot\Delta x); \qquad n = 0, 1, \cdots, D/\Delta x. \tag{9}$$

$\mu(x)$ obtained in this way[2] exhibits the following essential features, as shown in

[2] The method of Hosemann and Bagchi (1962, pp. 122–131) can be illustrated in a simple one-dimensional example. Assume a structure $\mu(x)$ to be given by five values $\mu(-D/2)$, $\mu(-D/4)$, $\mu(0)$, $\mu(D/4)$, $\mu(D/2)$. Since $\mu(x) = \mu(-x)$ and $p(x) = \mu(x) * \mu(-x)$, the convolution operation yields (equation 9)

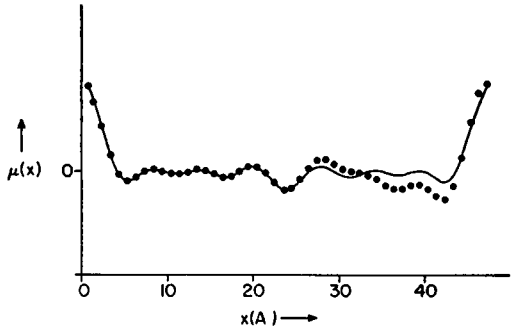

FIGURE 7 Electron density distribution $\mu(x)$ (in relative units) as obtained by a deconvolution of the Patterson function of a single unit cell. For the second half of the unit cell, from $D/2$ to D, a symmetric curve is drawn on the assumption that $\mu(x)$ in the first half of the unit cell is correct (see text). Points represent calculated values.

Fig. 7: (*a*) a narrow peak of high electron density at either edge of the unit cell, (*b*) an inner broad region with nearly constant electron density, and (*c*) a narrow region of approximately 4 A width in the center of the unit cell with an electron density which is lower than the average. These characteristics can be attributed to the layer of barium ions and adjacent carboxyl groups, the —CH_2— groups of the fatty acid chains and the terminal —CH_3 groups of the fatty acid chains, respectively. For comparison $\rho'(x)$ was calculated by a Fourier synthesis with the first nine reflections from a specimen with 60 unit cells. The two electron density functions agree very well, with the exception of rather deep minima immediately inside of the layer of barium ions in the Fourier synthesis, which are due to truncation artifacts. One may conclude, therefore, that the μ function meets criteria I and II, as does the function $\rho'(x)$ which is obtained by a Fourier synthesis.

It appears from Fig. 7 that $\mu(x)$ is not perfectly symmetric around the center of the unit cell. This may be due in part to a lack of precision in $P'(x)$ and $P_0(x)$. Probably a more important reason, however, is the choice of a finite sampling interval Δx for $p(x)$. The deconvolution operation starts at $x = 0$ and progresses through the unit cell up to $x = D$. Small errors will build up during the recursion process by which the deconvolution is performed. The values of $\mu(x)$ for the first half of the unit cell may be less affected by such errors. The deviation of $\mu(x)$ in the second half of the unit cell from a function which is symmetric around $D/2$ is probably due to a successive addition of small errors during the computation. On the

$$p(-D) = \mu(D/2)\cdot\mu(D/2)$$

$$p(-3D/4) = \mu(D/2)\cdot\mu(D/4) + \mu(D/4)\cdot\mu(D/2)$$

$$p(-D/2) = \mu(D/2)\cdot\mu(0) + \mu(D/4)\cdot\mu(D/4) + \mu(0)\cdot\mu(D/2)$$

and so on. Values of $p(x)$ are experimentally determined, and $\mu(D/2)$ can be obtained from $p(-D)$. The next step in the recursion process then gives $\mu(D/4)$ etc.

other hand, $\mu(x)$ is obtained by a straightforward analysis of experimental data and no assumptions enter into the calculation. The result may be considered to be satisfactory despite the slight asymmetry, since $\mu(x)$ in the present form shows the essential features of the structure. It can be used at least to select in an unambiguous manner the correct combination of phase angles and a Fourier synthesis can then be calculated in the conventional manner with diffraction from a specimen having many unit cells.

The electron density distribution obtained in this way is consistent with the observation that barium stearate multilayers give rise to identical diffraction phenomena whether the specimen is kept at 100% humidity or is vacuum dried. The amount of water present in the structure must be zero or very small. The narrow peaks of high electron density cannot be seen to separate from the edges of the unit cell even if $\rho'(x)$ is calculated to the highest resolution obtained. These peaks become narrower with increasing resolution. This tends to indicate that there is only one layer of barium ions between adjacent stearate layers. Even if no water space has to be allowed for in the unit cell, the unit cell dimension along the x-axis is too small to accommodate two fully extended fatty acid chains with 18 carbon atoms, unless the axis of the fatty acid chain is slightly tilted with regard to the x-axis. This postulate is verified by the observation that in exposures with a point-focused X-ray beam the peak at approximately 4.2 A due to the packing of the hydrocarbon chains (Vand, 1953; Engelman, 1970) spreads off the equator of the diffraction pattern.

CONCLUSIONS

It is usually thought that a specimen to be investigated by X-ray analysis must have a large number of unit cells if diffraction phenomena are to be observed. This, however, is not always true, and it can even be an advantage to use specimens with only a very small number of coherently diffracting unit cells. The information content of such diffraction patterns can be higher than that of the usual pattern obtained from specimens with many unit cells, and can be sufficient to allow a direct and unambiguous calculation of the electron density distribution in the specimen.

The electron density distribution of barium stearate multilayers can be determined based on diffraction from a specimen with two unit cells by a deconvolution of the Patterson function of a single unit cell. The result of this method is consistent with an independent, conventional Fourier synthesis calculated with an experimentally established phase sequence. There are two rather narrow peaks of high electron density in the unit cell at 0 and D, separated by a region of lower and constant electron density. In the center of the unit cell is a region of approximately 3 A width where the electron density is below average. This electron density distribution fits well with a physical model of barium stearate layers. The region of low and constant electron density corresponds to the inner hydrocarbon core of the bimolecular fatty acid leaflet. It is of interest that the region of the terminal —CH_3 groups of the fatty acid chains has a lower electron density than the chain of —CH_2—

groups. This indicates that the fatty acid chains do not interpenetrate. The narrow and high peaks of electron density at the edges of the unit cell must be caused by the layer of barium ions, since no other component has an electron density which is much higher than the average. No water space could be detected between the layers. It is likely that the barium ions bind to two carboxyl groups across the layers.

This work was supported by the U.S. Public Health Service grant GM 12202.

Received for publication 29 July 1970 and in revised form 9 October 1970.

REFERENCES

BLAUROCK, A. E. 1970. *Biophys. Soc. Annu. Meet. Abstr.* **10**:50a.
BLAUROCK, A. E., and C. R. WORTHINGTON. 1966. *Biophys. J.* **6**:305.
BLODGETT, K. B. 1935. *J. Amer. Chem. Soc.* **57**:1007.
ELLIOT, G., and C. R. WORTHINGTON. 1963. *J. Ultrastruct. Res.* **9**:166.
ENGELMAN, D. M. 1970. *J. Mol. Biol.* **47**:115.
FINEAN, J. B. 1953. *Biochim. Biophys. Acta.* **10**:371.
FRICKE, H. 1925. *Phys. Rev.* **26**:682.
GORTER, E., and F. GRENDEL. 1925. *J. Exp. Med.* **41**:439.
GRAS, W. J., and C. R. WORTHINGTON. 1969. *Proc. Nat. Acad. Sci. U.S.A.* **63**:233.
HOSEMANN, R., and S. N. BAGCHI. 1962. Direct Analysis of Diffraction by Matter. North Holland Publishing Co., Amsterdam.
JAMES, R. W. 1965. The Optical Principles of Diffraction of X-Rays. Cornell University Press, Ithaca, N.Y. 9.
LESSLAUER, W., and J. K. BLASIE. 1970. *Disc. Conf. Macromol.* Models Biopolymer Struct. Funct. Mariánské Lázně, Czechoslovakia.
Levine, Y. K., A. J. Bailey, and M. H. F. Wilkins. 1968. *Nature (London).* **220**:577.
LUZZATI, V. 1968. *In* Biological Membranes. D. Chapman, editor. Academic Press Inc. Ltd., London. 71.
SCHMITT, F. O., R. S. BEAR, and K. J. PALMER. 1941. *J. Cell. Comp. Physiol.* **18**:31.
SHER, I. H., and J. D. CHANLEY. 1955. *Rev. Sci. Instrum.* **26**:266.
STEIM, J. M., J. C. REINERT, M. E. TOURTELLOTTE, R. N. MCELHANEY, and R. L. RADER. 1969. *Proc. Nat. Acad. Sci. U.S.A.* **63**:109.
VAND, V. 1953. *Acta Crystallogr.* **6**:797.

APPENDIX

List of Symbols

$\rho_0(x)$, $\rho(x)$	Electron density distribution of single unit cell, total structure.
$\rho'(x)$	Resolution-limited electron density distribution obtained by Fourier synthesis.
$\mu(x)$	Electron density distribution obtained by a deconvolution of $P_0(x)$.
$F(x^*)$	Fourier transform of $\rho_0(x)$.
$I_{obs}(x^*)$	Observed diffracted intensity.
$P(x)$	Patterson function.
$P'(x)$	Generalized Patterson function obtained by an integral Fourier transform of observed intensity data, $I_{obs}(x^*)$.
$P_0(x)$	Patterson function of a single unit cell.
$z(x)$	Infinitely extended, one-dimensional δ function lattice of period D.

$s(x)$	Shape function with $s(x) = 1$ inside and $s(x) = 0$ outside the structure.
$\delta(x)$	Delta function (Dirac).
x	Axis normal to the plane of the layers.
$x^* = 2 \sin \theta/\lambda$	Reciprocal space coordinate.
D	Repeat distance along x.
N	Number of unit cells in the system.
$\Delta p/(1/D)$	Observed half-width of lamellar reflections in units of $1/D$.
h, h_{max}	Order of lamellar reflection, highest order observed.
$*$	Stands for a convolution operation.